Analytica Chimica Acta xxx (2015) xxx–xxx

Contents lists available at ScienceDirect

Analytica Chimica Acta

journal homepage: www.elsevier.com/locate/aca

Label-free colorimetric sensor for mercury(II) and DNA on the basis of mercury(II) switched-on the oxidase-mimicking activity of silver nanoclusters

Guang-Li Wang *, Lu-Yi Jin, Xiu-Ming Wu, Yu-Ming Dong, Zai-Jun Li

The Key Laboratory of Food Colloids and Biotechnology, Ministry of Education, School of Chemical and Material Engineering, Jiangnan University, Wuxi 214122, PR China

HIGHLIGHTS

- The oxidase-like activity of BSA-Ag NCs was "switched-on" selectively by Hg^{2+}.
- Hg^{2+} stimulated Ag NCs had a better affinity than HRP considering TMB as a substrate.
- The triggered enzyme mimicking activity was utilized to colorimetrically detect DNA.
- This colorimetric sensor for DNA was label-free, facile and fast.

GRAPHICAL ABSTRACT

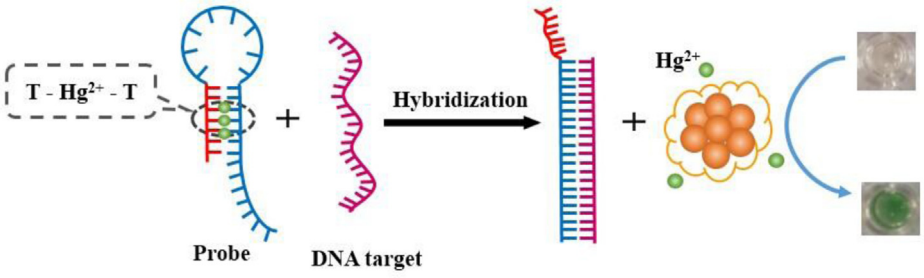

ARTICLE INFO

Article history:
Received 7 December 2014
Received in revised form 6 February 2015
Accepted 10 February 2015
Available online xxx

Keywords:
Enzyme mimetics
Silver nanoclusters
Mercury(II) detection
DNA detection
Catalytic activity

ABSTRACT

In this paper, a novel colorimetric biosensor for Hg^{2+} and DNA molecules is presented based on Hg^{2+} stimulated oxidase-like activity of bovine serum albumin protected silver clusters (BSA-Ag NCs). Under mild conditions, Hg^{2+} activated BSA-Ag NCs to show high catalytic activity toward the oxidation of 3,3′,5,5′-tetramethylbenzidine (TMB) using ambient dissolved oxygen as an oxidant. The oxidase-like activity of BSA-Ag NCs was "switched-on" selectively in the presence of Hg^{2+}, which permitted a novel and facile colorimetric sensor for Hg^{2+}. As low as 25 nmol L^{-1} Hg^{2+} could be detected with a linear range from 80 nmol L^{-1} to 50 mmol L^{-1}. In addition, the sensing strategy was also employed to detect DNA molecules. Hg^{2+} is known to bind very strongly and specifically with two DNA thymine bases (T) to form thymine–Hg^{2+}–thymine (T–Hg^{2+}–T) base pairs. The hairpin-structure was disrupted and Hg^{2+} ions were released after hybridization with the DNA target. By coupling the Hg^{2+} switched-on the oxidase-mimicking activity of BSA-Ag NCs, we developed a novel label-free strategy for facile and fast colorimetric detection of DNA molecules. More important, target DNA can be detected as low as 10 nmol L^{-1} with a linear range from 30 to 225 nmol L^{-1}. Compared with other methods, this method presents several advantages such as the independence of hydrogen peroxide, high sensitivity and good selectivity, avoiding any modification or immobilization of DNA, which holds a great potential of metal NCs for clinical application in biosensing and biotechnology.

1. Introduction

Colorimetric biosensing has been widely applied to the field of analysis and point-of-care testing due to its simplicity and practicality [1–3]. The challenge for colorimetric biosensing is

* Corresponding author. Tel.: +86 510 85917090; fax: +86 510 85917763.
E-mail address: glwang@jiangnan.edu.cn (G.-L. Wang).

http://dx.doi.org/10.1016/j.aca.2015.02.027
0003-2670/

transforming the detection signals into color changes which can be read by naked eyes. Nowadays, biosensors based on enzyme mimetics has emerged as a significant colorimetric tool for the detection of a variety of biomolecules, such as nucleotides [4], hydrogen peroxide (H_2O_2) [5,6], glucose [7,8], melamine [9], xanthine [10] and so on. Enzyme mimetics are a hot research area at present because they can overcome some intrinsic drawbacks of natural enzymes. For example, natural enzymes are easily denatured under harsh condition and digested by protease [11,12]. Additionally, the preparation, purification and storage condition for native enzymes are usually rigorous and expensive. These intrinsic drawbacks push people to explore new enzyme mimic substitutes which own the advantages of natural enzymes while avoid their disadvantages [13,14]. Gao et al. [15] reported that the magnetic Fe_3O_4 nanoparticles exhibited the intrinsic peroxidase-like activity, which opened the door for the development of nanoscaled materials as enzyme mimetics in bioanalysis field. Afterwards, increasing attentions have been devoted to the development of nanomaterial-based peroxidase mimics. Many nanostructures such as iron oxide [15], graphene oxide (GO) [16], carbon nanotubes [4], carbon dots [17], metal nanoparticles [8], and bimetallic alloy nanostructures [18] were found to possess peroxidase-like activity which could catalyze the oxidation of different typically chromogenic substrates using H_2O_2 as an oxidant. Compared to natural enzymes, these enzyme mimetics were found to possess several advantages such as controlled synthesis, readily preparation, high stability, low cost and so on. However, most of the currently developed nanoenzyme mimetics by use of destructive and unstable hydrogen peroxide as an oxidant makes their biological applications difficult. Thus, it is highly demanded that the development of novel enzyme mimics which have better biocompatibility [19].

Oxidases that can catalyze the oxidation of substrates by employing ambient oxygen as an electron acceptor are more facile and biocompatible, which not only play an important role in organic synthesis, but also hold good promising prospects for biosensor design. Unfortunately, little attempts have been made to fabricate colorimetric biosensors based on oxidase mimetics of nanomaterials. In an early report, cerium oxide nanoparticles were demonstrated to show pH dependent oxidase-like activity, which were used as a catalytic label for the detection of cancer biomarkers [20]. However, it was lately found that instead of being an oxidase mimic, nanoceria acted solely as an oxidizing agent in the oxidation of the organic substrates [21].

Molecule-like metal nanoclusters (NCs), with dimension about 1–3 nm, consisting of several to tens of metal atoms, have received enormous attention in recent years in the fields of sensing, catalysis, biological imaging and labeling due to their unique optical, electronic and physical properties [22–26]. Compared to nanoparticles, a high percentage of the metal content of metal NCs are exposed to the nanoparticle's surface. For instance, in a 2.0-nm NC, 50% of the metal atoms are exposed. Consequently, metal NCs are promising highly active catalysts [27]. However, few studies have reported using metal NCs to mimic oxidase [28].

In contrast to the fact that the fluorescence [29,30] and peroxide-like activity [31] of metal NCs could be seriously inhibited by metal ions, we found that mercury(II) ion selectively stimulated the oxidase-like activity of bovine serum albumin protected silver NCs (BSA-Ag NCs). The presence of Hg^{2+} enabled the BSA-Ag NCs to demonstrate high ability to catalyze the chromogenic reaction of the typical substrate, 3,3′,5,5′-tetramethylbenzidine (TMB), using ambient dissolved oxygen as an oxidant. Based on this phenomenon, we achieved a novel and facile colorimetric mercury(II) ion sensor. Besides, using the same sensing mechanism, we developed a label-free colorimetric method for the sensitive DNA detection employing Hg^{2+} stimulated oxidase activity of Ag NCs as a reporter event. The Hg^{2+} initially bound to capture DNA to form a hairpin-structured probe through thymine–Hg^{2+}–thymine (T–Hg^{2+}–T) mismatch formation. However, in the presence of the target DNA, the hairpin structure of the probe was opened through hybridization between the probe and target DNA and the sequestered Hg^{2+} ions was released. The released Hg^{2+} could trigger the oxidase-mimicking catalytic activity of BSA-Ag NCs, which catalyzed the chromogenic reaction for TMB. Compared with previously colorimetric reports, the current strategy holds many advantages. Firstly, unlike other peroxidase mimetics, the Hg^{2+}-stimulated Ag NCs demonstrated high enzyme-like activity without using destructive hydrogen peroxide as an oxidant, indicating their better biocompatibility for promising applications in biosensing systems. Secondly, the oxidase-like activity of BSA-Ag NCs inspired by Hg^{2+} was highly selective among other heavy metal ions. Thirdly, a label-free strategy was presented to detect DNA, preventing any modification or immobilization of DNA, thus making the developed method with the merits of simplicity, rapidity and cost-effectiveness.

2. Experimental details

2.1. Reagents

Bovine serum albumin (BSA, 96%), silver nitrate ($AgNO_3$), sodium borohydride ($NaBH_4$, 96%), 3,3′,5,5′-tetramethylbenzidine (TMB), 2,2-azino-bis(3-ethylbenzothiazoline-6-sulfonic acid) (ABTS), *o*-phenylenediamine (OPD), mercuric acetate ($Hg(Ac)_2$), isopropanol, tertiary butanol, N,N,N′,N′-tetramethylethylenediamine (TEMED, 98%), ammonium persulfate (APS, 98%) and bis-acrylamide were all acquired from Sinopharm Chemical Reagent Co., Ltd. (Shanghai, China). Superoxide dismutase (SOD) and acrylamide from bovine liver was purchased from Sigma–Aldrich (USA). All the DNA oligomers purified by HPLC and ethidium bromide (EB) were purchased from Sangon Biotechnology Co., Ltd. (Shanghai, China). All solutions were provided with ultrapure water (18.2 $M\Omega\,cm^{-1}$) acquired from a Healforce water purification system.

2.2. Apparatus

High resolution transmission electron microscopy (HRTEM) images of BSA-Ag NCs were captured by a JEOL JEM-2100 transmission electron microscope (Hitachi, Japan). The fluorescence spectra analysis was carried out on a Varian Cary Eclipse fluorescence spectrophotometer at room temperature. UV–vis absorption spectroscopic measurements were carried out using a TU-1901 spectrophotometer (Beijing Purkinje General Instrument Co., Ltd. China). The X-ray photoelectron spectra (XPS) were gained by an AXIS Ultra^{DLD} X-ray photoelectron spectroscopy (Shimadzu-Kratos, Japan). Polyacrylamide gel electrophoresis (PAGE) was conducted by a Molecular Imager Gel Doc XR (Bio-Rad USA). The detection of DNA by the absorption method was conducted on 96 well plates by the microplate reader (SpectraMax M5, USA).

2.3. Synthesis of BSA capped-Ag nanocluster (BSA-Ag NCs)

All glasswares were cleaned with Aqua Regia (volume ratio of HCl:HNO_3 3:1), and rinsed with ultrapure water thoroughly before use. The BSA-Ag NCs were prepared according to methods reported in literature [32], and the synthetic steps did some changes. Briefly, a 5 mL aqueous solution of $AgNO_3$ (5 mmol L^{-1}) was mixed with 5 mL of bovine serum albumin (BSA, 20 mg mL^{-1}) under vigorous stirring in dark at 0 °C. After 5 min, 30 μL of a freshly prepared aqueous solution of $NaBH_4$ (5 mmol L^{-1}) was introduced to reduce the Ag^+ ions to Ag(0) quickly with the color of the solution changed to pale brown. Five minutes later, 1.0 mol L^{-1} NaOH solution was

Please cite this article in press as: G.-L. Wang, et al., Label-free colorimetric sensor for mercury(II) and DNA on the basis of mercury(II) switched-on the oxidase-mimicking activity of silver nanoclusters, Anal. Chim. Acta (2015), http://dx.doi.org/10.1016/j.aca.2015.02.027

injected to adjust the pH of the reaction solution to around 8. Then, the reaction was allowed to continue for another 4 h. The final solution was then dialyzed in ultrapure water for 48 h to remove unreacted impurities.

2.4. Hg^{2+} stimulated oxidase-like activity of BSA-Ag NCs for the detection of Hg^{2+}

100 μL of BSA-capped Ag NCs (BSA-Ag NCs), a certain concentration of $Hg(A_C)_2$, 60 μL of 5.0×10^{-3} mol L^{-1} TMB and 100 μL of acetate buffer (0.2 mol L^{-1} HAc-NaAc, pH 4.0) were injected sequentially in a 1 mL standard colorimetric tube. Then, the mixed solution was diluted to volume with ultrapure water for absorption measurements.

2.5. DNA detection

Probes with three T–T mismatches and Hg^{2+} ions were mixed with a molar ratio of 1:3 and were plated in 96-well plates, and then incubated in Tris-HAc buffer (0.02 mol L^{-1}, pH 8) at room temperature for 30 min. Subsequently, different concentrations of DNA targets were added and allowed to hybridize under desired concentrations in Tris-HAc buffer (0.02 mol L^{-1}, pH 8) at room temperature for 2 h. Then, 40 μL of the BSA-Ag NCs and 80 μL of acetate buffer (HAc-NaAc, 0.2 mol L^{-1}, pH 4.0) were added. Afterward, 40 μL of 0.5 mmol L^{-1} TMB was added to react for 10 min to allow the development of the color. The absorbance of the oxidation product was recorded at 652 nm with a microplate reader. The process for detecting HIV-1 DNA was the same as the above procedures.

The sequences of the probe, perfect-match target, single-base mismatch target, and non-complementary target are listed below. The bases in bold are parts for the formation of an intra-molecular duplex through T–Hg^{2+}–T. The underlined bases are matched bases between the probe and the target. The bases without any mark are nonhybrization ones. The bases in italic are mismatched bases between the perfect-match target and the non-complementary target.

Probe: 5′-**GCTTTGA**CGTACGTA**TCTTTGC**ACCGACC-3′

Perfect-match target: 5′-GGTCGGTGCAAAGATACGTACGAG-GACA-3′

Single-base mismatch target: 3 5′-GGTCGGTGCAAAGCTACG-TACGAGGACA-3′

Non-complementary target: 4 5′-*CTAGCTGCATCCCGACGATC-GAAGAGTCTGATC*-3′

The sequences of probe-1, HIV-1 DNA and noncomplementary DNA are shown below.

Probe-1: 5′-**TGGTTTTA**TGCATCCAGGTCATG**TTATTCCA**AA-TATCTTCT-3′

5HIV-1 DNA: 5′-AGAAGATATTTGGAATAACATGACCTGGATGCA-3′

HIV-1 noncomplementary DNA: 6 5′-*CTAGCTGCATCCCGAC-GATCGAAGAGTCTGATC*-3′

2.6. Polyacrylamide gel electrophoresis (PAGE) analysis

DNA hybridization was confirmed by polyacrylamide gel electrophoresis (PAGE). 7 μL of DNA sample (10 μM) was mixed with 2 μL of 6× native loading buffer (20 mM phosphate buffer, 1.0 mM Mg^{2+}, pH 7.4, 50% glycerol, 0.25% bromphenol blue) and loaded into 12% native polyacrylamide gel. 1× TBE (90 mmol L^{-1} Tris, 90 mmol L^{-1} boric acid, 10 mmol L^{-1} EDTA, pH 8.0) was used as running buffer, and the electrophoresis voltage was set to 100 V. After running for 2 h, gels were stained with ethidium bromide (EB) for 30 min and imaged with a gel imaging system under UV excitation.

3. Results and discussion

3.1. Characterization of the BSA-Ag NCs

We used high resolution transmission electron microscopy (HRTEM) to characterize the formation of the BSA-Ag NCs. As shown in Fig. 1A, BSA-Ag NCs were monodispersed with an average

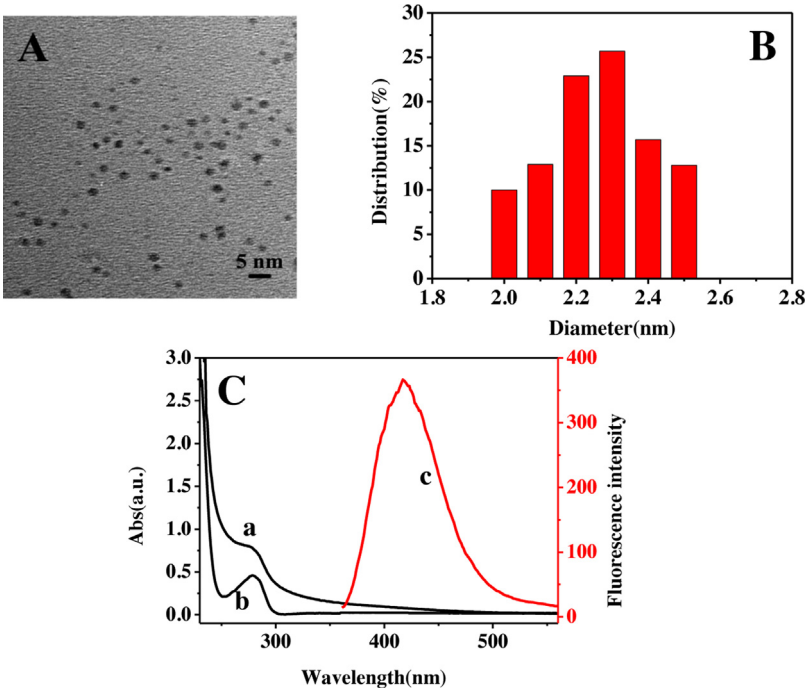

Fig. 1. HRTEM image (A), the histogram of the size distribution (B) and the absorption and fluorescence spectra (C) of BSA-Ag NCs. Fluorescence spectra of BSA-Ag NCs (red line, right axis, curve c) and UV–vis absorption spectra (black line, left axis) of BSA (curve a), BSA-Ag NCs (curve b). (For interpretation of the references to color in this figure legend, the reader is referred to the web version of this article.)

Please cite this article in press as: G.-L. Wang, et al., Label-free colorimetric sensor for mercury(II) and DNA on the basis of mercury(II) switched-on the oxidase-mimicking activity of silver nanoclusters, Anal. Chim. Acta (2015), http://dx.doi.org/10.1016/j.aca.2015.02.027

size of approximately 2–2.5 nm. The histogram of the size distribution of BSA-Ag NCs is shown in Fig. 1B. As shown in Fig. 1C (curve b), the UV–vis absorption spectra of BSA had no obvious absorption peak between 300–500 nm but only a characteristic absorption peak at about 270 nm. In contrast, besides the characteristic absorption peak at about 270 nm, the UV–vis absorption spectra of BSA-Ag NCs also exhibited a wide absorption between 300 and 500 nm, which was due to the formation of Ag NCs embedded in BSA (Fig. 1C, curve a). The BSA-Ag NCs introduced strong fluorescence emission at 420 nm with excitation at 310 nm (Fig. 1C, curve c). Photoluminescence is an important property of NCs resulted from quantum confinement and discrete energy levels of NCs [33].

We also examined the surface Ag content of the as-prepared samples by X-ray photoelectron spectroscopy (Fig. S1). The XPS spectra showed that the BSA acted as a ligand on the surface of Ag NCs (Fig. S1A). The valence states of silver in the BSA-Ag NCs were also analyzed and the high-resolution spectrum of Ag 3d was provided in Fig. S1B. The spectrum showed the Ag 3d dividing into Ag 3d3/2 (373.2 eV) and Ag 3d5/2 (367.2 eV) peaks with a peak separation of 6.0 eV and confirmed that the valence state of silver element was Ag(0) [34].

NCs was stimulated immediately and catalyzed the chromogenic reaction of TMB (Fig. 2c), which produced the oxidized TMB (oxTMB) with a characteristic absorbance at 652 nm and simultaneously generated a blue-green color of oxTMB (Fig. 2). To further characterize the oxidase-like activity of the Hg^{2+} stimulated Ag NCs, other typical peroxidase substrates including 2,2′-azino-bis (3-ethylbenzothiazoline-6-sulfonic acid) (ABTS) and *o*-phenylenediamine (OPD) were used in place of TMB. It was found that OPD could also be oxidized to its oxidation product by forming an orange color. However, after adding ABTS, the reaction solution produced flocculent precipitate. This indicated that ABTS was not a suitable chromogenic substrate of Hg^{2+} stimulated Ag NCs. After bubbling pure nitrogen into the reaction solution to eliminate dissolved oxygen, the catalytic reaction activity for TMB oxidation through the BSA-Ag NCs by the use of Hg^{2+} decreased obviously (Fig. S2) indicating that the essence of the oxidase-like activity of Hg^{2+}-Ag NCs employing oxygen as a green oxidant. That is, the oxidation of TMB was originated from the catalytic ability of the catalyst to activate dissolved oxygen but not the direct reaction between BSA-Ag NCs or Hg^{2+} with TMB. The oxidase-like activity of Hg^{2+} triggered BSA-Ag NCs for the oxidation of TMB can be depicted by the following Eq. (1).

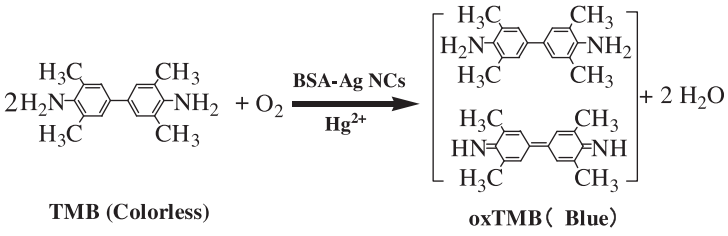

(1)

3.2. Hg^{2+} stimulated oxidase-like activity of BSA-Ag NCs

To investigate the Hg^{2+} stimulated catalytic activity of BSA-Ag NCs, 3,3′,5,5′-tetramethylbenzidine (TMB) as a representative chromogenic substrate was chosen. TMB has been widely used to demonstrate the oxidase- or peroxidase-like activities of natural enzymes or enzyme mimetics [15,35]. In the presence of ambient dissolved oxygen, the chromogenic substrate of TMB was not catalyzed oxidation by BSA-Ag NCs or Hg^{2+} alone (Fig. 2a and b). However, after the addition of Hg^{2+}, the catalytic activity of BSA-Ag

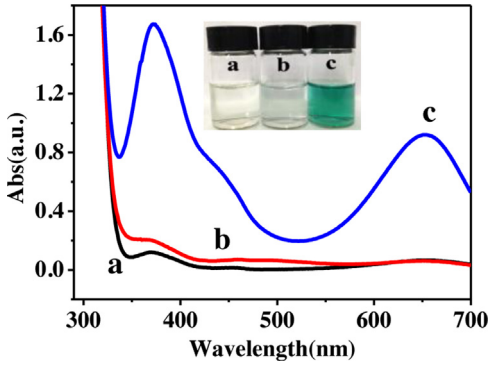

Fig. 2. UV–vis spectra of (a) BSA-Ag NCs + TMB; (b) Hg^{2+} + TMB; (c) BSA-Ag NCs + Hg^{2+} + TMB; inset image is the corresponding color of the above solutions. All the above solutions were prepared in acetate buffer with pH of 4.0. (For interpretation of the references to color in the text, the reader is referred to the web version of this article.)

3.3. Influence factors for the catalytic activity of Hg^{2+} stimulated BSA-Ag NCs

The relative catalytic activity of Hg^{2+} stimulated BSA-Ag NCs relied on temperature and solution pH like the native enzymes. Here, we monitored the relative catalytic activity of Hg^{2+} stimulated BSA-Ag NCs while changing the temperature from 0 to 70 °C and the pH from 2 to 12. We compared the results with the activity of HRP over the same range of parameters. The effects of these two parameters on the relative catalytic activity of TMB oxidation are shown in Fig. S3. We found an optimal pH of 4.0 and optimal temperature of 10 °C for Hg^{2+} stimulated Ag NCs. It should be pointed out that the BSA-Ag NCs had improved stability than natural HRP at lower pH and lower temperatures, indicating that BSA-Ag NCs as enzyme mimetics showed better stability against stringent conditions than the natural enzyme.

Similar to the nature enzyme catalyzed reaction, a strong dependence was found between initial reaction rate and the concentration of the substrate – TMB (Fig. S4). We further investigated the catalytic property of Hg^{2+} stimulated BSA-Ag NCs using steady-state kinetics. The kinetic data were obtained by varying the substrate's concentrations. Typical Michaelis–Menten curves were observed for Hg^{2+} stimulated BSA-Ag NCs within an appropriate range of TMB concentrations (Fig. S5). The Michaelis–Menten constant (K_m), which is an indicator of enzyme affinity for its substrate, was obtained by using Lineweaver–Burk plot: $v = V_{max} \times [S]/(K_m + [S])$, where v, V_{max}, $[S]$ and K_m refer to the initial velocity, the maximum reaction velocity, the concentration of the substrate and Michaelis constant, respectively [36]. Under the optimized conditions, the apparent Michaelis constant (K_m)

(at 10 °C) and the maximum reaction rate value (V_{max}) of Hg^{2+} stimulated BSA-Ag NCs with TMB as substrate were 119 μM and 214 nM S^{-1}, respectively. The apparent K_m value of the Hg^{2+} stimulated BSA-Ag NCs with TMB as the substrate was lower than that of HRP (K_m = 0.434 mM, at 40 °C) [15], indicating that Hg^{2+} stimulated Ag NCs had a better affinity than HRP considering TMB as a substrate.

3.4. Reaction mechanism

In order to manifest the mechanism of the Hg^{2+} stimulated oxidase-like activity of BSA-Ag NCs, the surface Ag content of the as-prepared BSA-Ag NCs after the addition of Hg^{2+} was also investigated by XPS (Fig. S6). The binding of Hg^{2+} to BSA-Ag clusters was confirmed (Fig. S6A). The peak appeared in Fig. S6B was attributed to Hg 4f7/2 (101.2), corresponding to Hg(II). The full width at half maximum (FWHM) and peak area of Ag(0) obviously altered in the presence of Hg^{2+} (Fig. S7). The results of XPS showed that Hg^{2+} could bind with Ag(0) on the surfaces of BSA-Ag NCs and change the binding energy of Ag(0). The change in binding energy caused a change in the surface character and catalytic activity of BSA-Ag NCs.

In order to prove the catalytic reaction mechanism, it is essential to illustrate the nature of reactive oxygen species (ROS) produced from the decomposition of O_2 catalyzed by Hg^{2+}-Ag NCs. To further evaluate the effect of the ROS, we added radical inhibitors into the system of Hg^{2+}-Ag NCs. Isopropanol or *t*-butanol can quench •OH in solution [37,38]. As shown in Fig. S8, isopropanol or *t*-butanol quencher exhibited no influence on the oxidation of TMB under Hg^{2+}-Ag NCs, which demonstrated that •OH was not the main ROS. While the introduction of the $O_2^{\bullet-}$ scavenger of superoxide dismutase (SOD) [38,39] restrained the oxidation of TMB obviously, suggesting that superoxide anion ($O_2^{\bullet-}$) played a significant role in the oxidation of TMB. In the experiment, the Hg^{2+}-Ag NCs activated molecule oxygen to generate $O_2^{\bullet-}$ and contributed to the oxidation of TMB (Scheme 1).

3.5. Analytical performance for the detection of mercury(II)

Mercury(II) is an extremely poisonous and harmful heavy metal ion which can be accumulated in human body, and long-time exposure to even low concentrations of mercury could causes severe damages to various organs [40]. Therefore, it is highly necessary to find a simple and inexpensive method for the detection of Hg^{2+}. So far, many fluorescent or colorimetric sensors based on metal NCs or quantum dots (QDs) [41] for the detection of Hg^{2+} were reported [29,31]. It found that Hg^{2+} could quench the fluorescence of QDs/metal NCs or the peroxidase-like activity of metal NCs strongly. Hence, most Hg^{2+} sensors involving metal NCs were "switch-off" sensors [29,42–44]. However, some shortcomings restrict the applications of "switch-off" sensors, such as large background variation and susceptibility to false signals. Based on the specific enhancing effect of mercury(II) on the oxidase-like catalytic activity of BSA-Ag NCs, we developed a facile and novel "switch-on" colorimetric sensing for Hg^{2+}. Under the optimal experimental conditions, the calibration curve of the absorbance of oxTMB at 652 nm against the Hg^{2+} concentration was linear in a range from 8×10^{-8} to 5×10^{-5} mol L^{-1} with a detection limit of 2.5×10^{-8} mol L^{-1} (Fig. 3A). The detection limit of the method was lower than the maximum mercury level defined for drinking water by the World Health Organization (WHO) (~30 nmol L^{-1}) [45]. Thus, our method was potentially applicable to qualitative and semi-quantitative detection. Our research can be also applied for fast naked-eyed screening without any instrumentation.

By adopting TMB chromogenic reaction to evaluate the oxidase-like activity of BSA-Au NCs stimulated by Hg^{2+}, effects of other common metal ions on the catalytic activity were also investigated. As shown in Fig. 3B, the catalytic effect of BSA-Ag NCs was stimulated by Hg^{2+} selectively, and 10 μM of Ag^+, Cd^{2+}, Pb^{2+}, Ca^{2+}, Cu^{2+},Ni^{2+}, Co^{2+}, Zn^{2+},Al^{3+}, Mn^{2+}, Fe^{3+}, Fe^{2+}, Na^+ showed no evident effect on the oxidase-like activity of BSA-Ag NCs. The result displayed that the stimulating effect of Hg^{2+} on the oxidase-like activity of BSA-Ag NCs was highly selective.

3.6. DNA detection

The label-free detection strategy has gained much interest because it can provide fast and cost-effective DNA detection [46]. Herein, a label-free colorimetric method was developed for the sensitive detection of DNA. We used Hg^{2+} stimulated oxidase-like activity of Ag NCs to detect DNA. At first, mercury ions (Hg^{2+}) were sequestered in the hairpin-structured probe through T–Hg^{2+}–T mismatch formation. Because the formation of the T–Hg^{2+}–T base pair was highly efficient and specific to T–T mismatch and Hg^{2+} [47]. Upon hybridization with the DNA target, the hairpin was disrupted and Hg^{2+} was released [48]. Afterward, BSA-Ag NCs were added and incorporated into the released Hg^{2+} spontaneously, catalyzed the chromogenic reaction of TMB. Successful hybridization between the probe and the target DNA was confirmed by native polyacrylamide gel electrophoresis (PAGE) (Fig. S9). Relative to those of perfect-match target alone (lane 1), single-base mismatch target alone (lane 2), non-complementary target alone (lane 3), or probe alone (lane 4), obvious bands with lower mobility was observed in lane 5 and lane 6, indicating that the probe and the perfect-match target or single-base mismatch target formed a stable duplex structure. The perfect-match target had a higher affinity with the probe than the single-base mismatch target, as can be judged from the complete disappearance of the probe band and the formation of a brighter band due to hybridization. While non-complementary target could not hybridize with the probe (lane 7). The reaction mechanism for detecting the target DNA is demonstrated as Scheme 2.

As a proof-of-concept study, we firstly used a scrambled DNA (5′-GGTCGGTGCAAAGATACGTACGAGGACA-3′) as a target. The probe (5′-**GCTTTGA**CGTACGTA**TCTTTGC**ACCGACC-3′) contained a

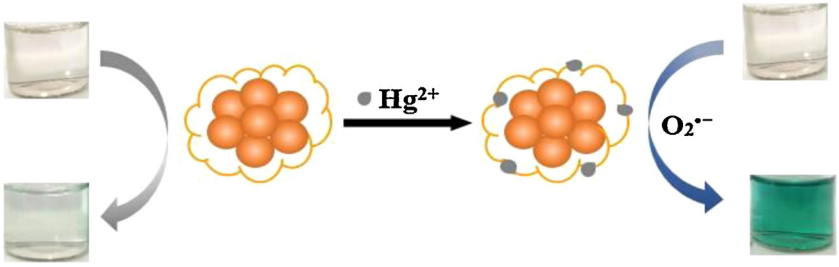

Scheme 1. The Hg^{2+} stimulated oxidase-like activity of BSA-Ag NCs.

Please cite this article in press as: G.-L. Wang, et al., Label-free colorimetric sensor for mercury(II) and DNA on the basis of mercury(II) switched-on the oxidase-mimicking activity of silver nanoclusters, Anal. Chim. Acta (2015), http://dx.doi.org/10.1016/j.aca.2015.02.027

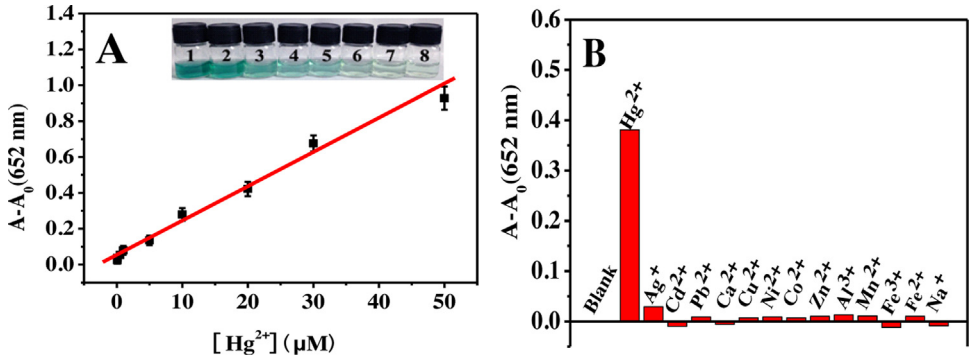

Fig. 3. Linear calibration plot for Hg^{2+} detection (A). The inset shows the corresponding color change of TMB catalytically oxidized by BSA-Ag NCs and various concentrations of Hg^{2+} (from 1 to 8, the concentrations of Hg^{2+} were: 5×10^{-5}, 3×10^{-5}, 2×10^{-5}, 5×10^{-6}, 1×10^{-6}, 5×10^{-7}, 1×10^{-7}, 8×10^{-8} mol L^{-1}). Catalytic activity of BSA-Ag NCs for the oxidation of TMB stimulated by various metal ions (B). A_0 is the absorbance of oxTMB at 652 nm in the presence of BSA-Ag NCs, and A is the absorbance of oxTMB at 652 nm in the presence of BSA-Ag NCs and different metal ions. The error bars indicate relative standard deviation of four repeated experiments.

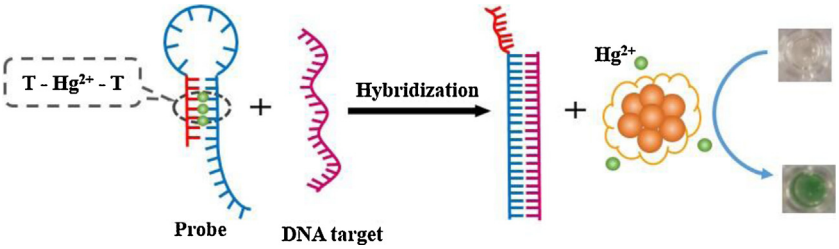

Scheme 2. Schematic illustration of label-free DNA detection based on BSA-Ag NCs.

domain (underlined) that was complementary to the target DNA and another domain (bolded) that formed an intra-molecular duplex containing three T–T mismatches. We mixed the probe DNA and Hg^{2+} with a molar ratio of 1:3. Then, each probe molecule would generate three T–Hg^{2+}–T base pairs. Afterwards, the probe was hybridized with different concentrations of target DNA. The released Hg^{2+} stimulated the catalytic activity of BSA-Ag NCs and catalyzed the chromogenic reaction of TMB with a significant absorbance at 652 nm. There was a good linear relationship between the change of the absorbance at 652 nm and the concentration of target DNA ranging from 30 to 225 nM (Fig. 4) and the detection limit was estimated to be 10 nM.

We hoped that the method would have good selectivity for the DNA target through the basic competition between unimolecular hairpin reaction and probe-target hybridization of probe-Hg^{2+}. The capability of this method in the single nucleotide polymorphism (SNP) detection was investigated. Three targets including perfect-match target, single-base mismatch target, and noncomplementary target (see Section 2 for sequences) were added against the probe with certain probe/target ratios (1:3). Fig. 5 compared the absorption spectrum changes of probe-Hg^{2+} in the presence of the same concentration of perfect-match target, single-base mismatch target, and noncomplementary target. The absorption signal change by single-base mismatch target was about 51.2% compared with same amount of perfect-match target. The results revealed that the single-base mismatch detection ability of probe-Hg^{2+} was comparable to or better than that of common MB, for which single-base mismatches result in a 50–90% signal change [49–51]. These results suggested that this method could be used to detect DNA sequences containing single mutations without any chemical modification of the DNA probe.

Subsequently, we detected clinical significant DNA fragments by this method from human immunodeficiency virus HIV-1 DNA. HIV-1 DNA fragment was a statistically unique sequence from HIV [52]. The sequences of probe-1, HIV-1 DNA and HIV-1 noncomplementary DNA were displayed in Section 2. The probe-1 was designed to detect HIV-1 DNA and it contained three T–T mismatches in each stem. For HIV-1 detection, 1 μM probe-1 (3 μM Hg^{2+}) was mixed with HIV-1 DNA target or HIV-1 noncomplementary DNA with 1:1 molar ratio. Fig. S10 compared the absorption spectrum changes of probe-1-Hg^{2+} in the presence of the same concentration of HIV-1 DNA and HIV-1 noncomplementary DNA. HIV-1 noncomplementary DNA had no influence on detecting HIV-1 DNA. There was a good linear relationship between the change of the absorbance at 652 nm and the HIV-1 DNA target concentration ranging from 45 to 225 nM (Fig. S11). The detection limit was estimated to be 20 nM. These results suggested that it had high selectivity and sensitivity to detect disease-relevant DNA sequences. This fast and facile method could potentially be applied to clinic detection and would provide great promise for DNA assay.

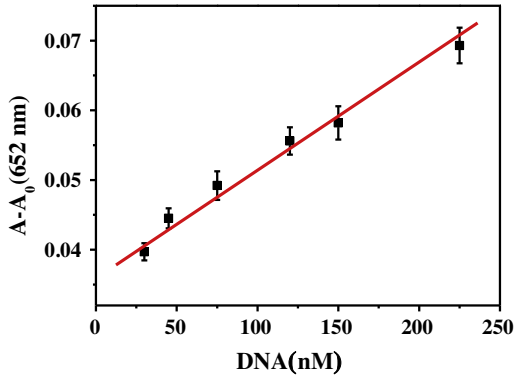

Fig. 4. The linear relationship between the absorption change (A–A_0) of oxTMB at 652 nm and the concentrations of target DNA. A_0 is the absorbance of oxTMB at 652 nm in the presence of BSA-Ag NCs, and A is the absorbance of oxTMB at 652 nm in the presence of BSA-Ag NCs and target DNA with different concentrations. The error bars indicate relative standard deviation of four repeated experiments.

Please cite this article in press as: G.-L. Wang, et al., Label-free colorimetric sensor for mercury(II) and DNA on the basis of mercury(II) switched-on the oxidase-mimicking activity of silver nanoclusters, Anal. Chim. Acta (2015), http://dx.doi.org/10.1016/j.aca.2015.02.027

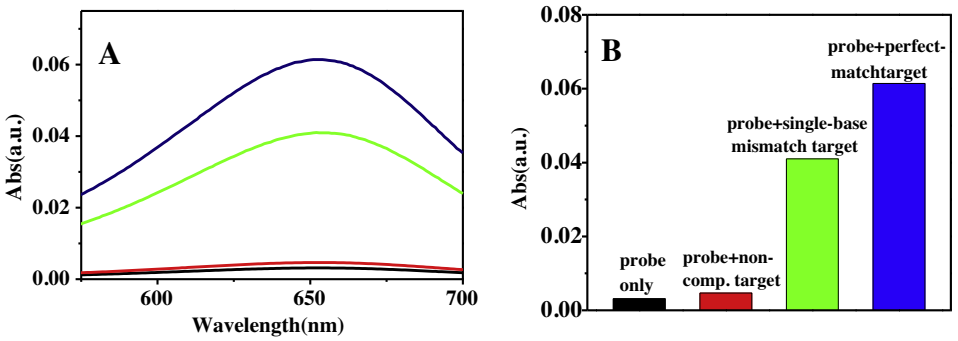

Fig. 5. Detection of perfect-match, single-base mismatch target and noncomplementary target. UV–vis spectra (A) and bar diagram (B) of BSA-Au NCs mixed probe-Hg^{2+} only (black) and probe-Hg^{2+} with perfect-match target (blue), single-base mismatch target (green), and noncomplementary target (red). (For interpretation of the references to color in this figure legend, the reader is referred to the web version of this article.)

4. Conclusions

To sum up, Hg^{2+} could stimulate the oxidase-like activity of BSA-Ag NCs selectively and sensitively, which enabled a sensitive colorimetric assay for Hg^{2+}. The Hg^{2+} stimulated oxidase-like activity of BSA-Ag NCs was attributed to that Hg^{2+} bound on the surface of BSA-Au NCs, changing the surface character and promoting the generation of superoxide anion for TMB oxidation. The Hg^{2+} stimulated oxidase-like activity of BSA-Ag NCs was further extended to a novel general strategy for facile and fast colorimetric detection of DNA molecules in solution. The method did not need any chemical labeling or modification of the DNA probe and also could be potentially used for the detection of clinical significant DNA targets. Therefore, the colorimetric method for DNA detection was much more convenient and cost-effective than the traditional FRET-based MBs.

Acknowledgements

This work was supported by the National Natural Science Foundation of China (21275065, 21005031), the Fundamental Research Funds for the Central Universities (JUSRP51314B) and the Opening Foundation of the State Key Laboratory of Analytical Chemistry for Life Science of Nanjing University (KLACLS1008).

Appendix A. Supplementary data

Supplementary data associated with this article can be found, in the online version, at http://dx.doi.org/10.1016/j.aca.2015.02.027.

References

[1] S.K. Ghosh, T. Pal, Interparticle coupling effect on the surface plasmon resonance of gold nanoparticles: from theory to applications, Chem. Rev. 107 (2007) 4797–4862.
[2] M.-C. Daniel, D. Astruc, Gold nanoparticles: assembly, supramolecular chemistry, quantum-size-related properties, and applications toward biology, catalysis, and nanotechnology, Chem. Rev. 104 (2004) 293–346.
[3] M. De, P.S. Ghosh, V.M. Rotello, Applications of nanoparticles in biology, Adv. Mater. 20 (2008) 4225–4241.
[4] Y. Song, X. Wang, C. Zhao, K. Qu, J. Ren, X. Qu, Label-free colorimetric detection of single nucleotide polymorphism by using single-walled carbon nanotube intrinsic peroxidase-like activity, Chem. Eur. J. 16 (2010) 3617–3621.
[5] J. Sun, J. Ge, W. Liu, M. Lan, H. Zhang, P. Wang, Y. Wang, Z. Niu, Multi-enzyme coembedded organic–inorganic hybrid nanoflowers: synthesis and application as a colorimetric sensor, Nanoscale 6 (2014) 255–262.
[6] Z. Chen, J.-J. Yin, Y.-T. Zhou, Y. Zhang, L. Song, M. Song, S. Hu, N. Gu, Dual enzyme-like activities of iron oxide nanoparticles and their implication for diminishing cytotoxicity, ACS Nano 6 (2012) 4001–4012.
[7] Z.H. Dai, S.H. Liu, J.C. Bao, H.X. Ju, Nanostructured FeS as a mimic peroxidase for biocatalysis and biosensing, Chem. Eur. J. 15 (2009) 4321–4326.
[8] Y. Jv, B.X. Li, R. Cao, Positively-charged gold nanoparticles as peroxidiase mimic and their application in hydrogen peroxide and glucose detection, Chem. Commun. 46 (2010) 8017–8019.
[9] N. Ding, N. Yan, C. Ren, X. Chen, Colorimetric determination of melamine in dairy products by Fe_3O_4 magnetic nanoparticles-H_2O_2-ABTS detection system, Anal. Chem. 82 (2010) 5897–5899.
[10] X.X. Wang, Q. Wu, Z. Shan, Q.M. Huang, BSA-stabilized Au clusters as peroxidase mimetics for use in xanthine detection, Biosens. Bioelectron. 26 (2011) 3614–3619.
[11] J.X. Xie, X.D. Zhang, H. Wang, H.Z. Zheng, Y.M. Huang, Analytical and environmental applications of nanoparticles as enzyme mimetics, TrAc Trend Anal. Chem. 39 (2012) 114–129.
[12] X.N. Hu, J.B. Liu, S. Hou, T. Wen, W.Q. Liu, K. Zhang, W.W. He, Y.L. Ji, H.X. Ren, Q. Wang, X.C. Wu, Research progress of nanoparticles as enzyme mimetics, Sci. China Phys. Mech. Astron. 54 (2011) 1749–1756.
[13] J. Kuwabara, C.L. Stern, C.A. Mirkin, A coordination chemistry approach to a multieffector enzyme mimic, J. Am. Chem. Soc. 29 (2007) 10074–10075.
[14] H. Wei, E. Wang, Nanomaterials with enzyme-like characteristics (nanozymes): next-generation artificial enzymes, Chem. Soc. Rev. 42 (2013) 6060–6093.
[15] L.Z. Gao, J. Zhuang, L. Nie, J.B. Zhang, Y. Zhang, N. Gu, T.H. Wang, J. Feng, D.L. Yang, S. Perrett, X.Y. Yan, Intrinsic peroxidase-like activity of ferromagnetic nanoparticles, Nat. Nanotechnol. 2 (2007) 577–583.
[16] Y.J. Song, K.G. Qu, C. Zhao, J.S. Ren, X.G. Qu, Graphene oxide: intrinsic peroxidase catalytic activity and its application to glucose detection, Adv. Mater. 22 (2010) 2206–2210.
[17] W. Shi, Q. Wang, Y. Long, Z. Cheng, S. Chen, H. Zheng, Y. Huang, Carbon nanodots as peroxidase mimetics and their applications to glucose detection, Chem. Commun. 47 (2011) 6695–6697.
[18] W. He, X. Wu, J. Liu, X. Hu, K. Zhang, S. Hou, W. Zhou, S. Xie, Design of AgM bimetallic alloy nanostructures (M = Au, Pd Pt) with tunable morphology and peroxidase-like activity, Chem. Mater. 22 (2010) 2988–2994.
[19] G.L. Wang, X.F. Xu, L. Qiu, Y.M. Dong, Z.J. Li, C. Zhang, Dual responsive enzyme mimicking activity of AgX (X = Cl, Br I) nanoparticles and its application for cancer cell detection, ACS Appl. Mater. Interfaces 6 (2014) 6434–6442.
[20] A. Asati, C. Kaittanis, S. Santra, J.M. Perez, pH-tunable oxidase-like activity of cerium oxide nanoparticles achieving sensitive fluorigenic detection of cancer biomarkers at neutral pH, Anal. Chem. 83 (2011) 2547–2553.
[21] Y.F. Peng, X.J. Chen, G.S. Yia, Z.Q. Gao, Mechanism of the oxidation of organic dyes in the presence of nanoceria, Chem. Commun. 47 (2011) 2916–2918.
[22] J. Zheng, P.R. Nicovich, R.M. Dickson, Highly fluorescent noble metal quantum dots, Annu. Rev. Phys. Chem. 58 (2007) 409–431.
[23] G. Ramakrishna, O. Varnavski, J. Kim, D. Lee, T. Goodson, Quantum-sized gold clusters as efficient two-photon absorbers, J. Am. Chem. Soc. 130 (2008) 5032–5033.
[24] J.H. Yu, S. Choi, R.M. Dickson, Shuttle-based fluorogenic silver-cluster biolabels, Angew. Chem. Int. Ed. 121 (2009) 324–326.
[25] W.W. Guo, J.P. Yuan, Q.Z. Dong, E.K. Wang, Highly sequence-dependent formation of fluorescent silver nanoclusters in hybridized DNA duplexes for single nucleotide mutation identification, J. Am. Chem. Soc. 132 (2010) 932–934.
[26] M.S. Devadas, S. Bairu, H. Qian, E. Sinn, R. Jin, G. Ramakrishna, Temperature-dependent optical absorption properties of monolayer-protected Au25 and Au38 clusters, J. Phys. Chem. Lett. 2 (2011) 2752–2758.
[27] A.A. Herzing, C.J. Kiely, A.F. Carley, P. Landon, G.J. Hutchings, Identification of active gold nanoclusters on iron oxide supports for CO oxidation, Science 321 (2008) 1331–1335.
[28] C.J. Yu, T.H. Chen, J.Y. Jiang, W.L. Tseng, Lysozyme-directed synthesis of platinum nanoclusters as a mimic oxidase, Nanoscale 6 (2014) 9618–9624.
[29] J.P. Xie, Y.G. Zheng, J.Y. Ying, Highly selective and ultrasensitive detection of Hg^{2+} based on fluorescence quenching of Au nanoclusters by Hg^{2+}–Au^{+} interactions, Chem. Commun. 46 (2010) 961–963.
[30] G.F. Wang, G. Xu, Y.H. Zhu, X.J. Zhang, A turn-on carbon nanotube–Ag nanoclusters fluorescent sensor for sensitive and selective detection of Hg^{2+} with cyclic amplification of exonuclease III activity, Chem. Commun. 50 (2014) 747–750.

Please cite this article in press as: G.-L. Wang, et al., Label-free colorimetric sensor for mercury(II) and DNA on the basis of mercury(II) switched-on the oxidase-mimicking activity of silver nanoclusters, Anal. Chim. Acta (2015), http://dx.doi.org/10.1016/j.aca.2015.02.027

[31] R. Zhu, Y. Zhou, X.L. Wang, L.P. Liang, Detection of Hg^{2+} based on the selective inhibition of peroxidase mimetic activity of BSA-Au clusters, Talanta 17 (2013) 127–132.
[32] X.L. Guével, B. Hötzer, G. Jung, K. Hollemeyer, V. Trouillet, M. Schneider, Formation of fluorescentmetal (Au, Ag) nanoclusters capped in bovine serum albumin followed by fluorescence and spectroscopy, J. Phys. Chem. C 115 (2011) 10955–10963.
[33] T.Y. Zhou, L.P. Lin, M.C. Rong, Y.Q. Jiang, X. Chen, Silver–gold alloy nanoclusters as a fluorescence-enhanced probe for aluminum ion sensing, Anal. Chem. 85 (2013) 9839–9844.
[34] E. Nehlig, R. Schneider, L. Vidal, G. Clavier, L. Balan, Silver nanoparticles coated with thioxanthone derivative as hybrid photoinitiating systems for free radical polymerization, Langmuir 28 (2012) 17795–17802.
[35] W.W. He, Y. Liu, J.S. Yuan, J.J. Yin, X.C. Wu, X.N. Hu, K. Zhang, J.B. Liu, C.Y. Chen, Y.L. Ji, Y.T. Guo, Au@Pt nanostructures as oxidase and peroxidase mimetics for use in immunoassays, Biomaterials 32 (2011) 1139–1147.
[36] L. Michaelis, M.L. Menten, Die Kinetik der Invertinwirkung, Biochemistry Z 49 (1913) 333–369.
[37] C.H. An, J.Z. Wang, C. Qin, W. Jiang, S.T. Wang, Y. Li, Q.H. Zhang, Synthesis of Ag@AgBr/AgCl heterostructured nano-cashews with enhanced photoca talytic performance via anion exchange, J. Mater. Chem. 22 (2012) 13153–13158.
[38] J. Cao, B.Y. Xu, B.D. Luo, H.L. Lin, S.F. Chen, Preparation, characterization and visible-light photocatalytic activity of AgI/AgCl/TiO_2, Appl. Surf. Sci. 257 (2011) 7083–7089.
[39] W. Wang, X.P. Jiang, K.Z. Chen, Iron phosphate microflowers as peroxidase mimic and superoxide dismutase mimic for biocatalysis and biosensing, Chem. Commun. 48 (2012) 7289–7291.
[40] X. Xue, F. Wang, X. Liu, One-Step Room temperature, colorimetric detection of mercury (Hg^{2+}) using DNA/nanoparticle conjugates, J. Am. Chem. Soc. 130 (2008) 3244–3245.
[41] L. Zhou, Y.H. Lin, Z.Z. Huang, J.S. Ren, X.G. Qu, Carbon nanodots as fluorescence probes for rapid sensitive, and label-free detection of Hg^{2+} and biothiols in complex matrices, Chem. Commun. 48 (2012) 1147–1149.
[42] C.L. Guo, J. Irudayaraj, Fluorescent Ag clusters via a protein-directed approach as a Hg(II) ion sensor, Anal. Chem. 83 (2011) 2883–2889.
[43] W.W. Guo, J.P. Yuan, E.K. Wang, Oligonucleotide-stabilized Ag nanoclusters as novel fluorescence probes for the highly selective and sensitive detection of the Hg^{2+} ion, Chem. Commun. 45 (2009) 3395–3397.
[44] G.Y. Lan, W.Y. Chen, H.T. Chang, Control of synthesis and optical properties of DNA templated silver nanoclusters by varying DNA length and sequence, RSC Adv. 1 (2011) 802–807.
[45] World Health Organization, Guidelines for Drinking-Water Quality: Incorporating 1st and 2nd Addenda, third ed., Recommendations, vol. 1, World Health Organization, Geneva, 2010 http://www.who.int/water_sanitation_health/dwq/fulltext.pdf (accessed 11.10.).
[46] E.G. Ju, X.J. Yang, Y.H. Lin, F. Pu, J.S. Ren, X.G. Qu, Exonuclease-aided amplification for label-free and fluorescence turn-on DNA detection based on aggregation-induced quenching, Chem. Commun. 48 (2012) 11662–11664.
[47] Y. Miyake, H. Togashi, M. Tashiro, H. Yamaguchi, S. Oda, M. Kudo, Y. Tanaka, Y. Kondo, R. Sawa, T. Fujimoto, T. Machinami, A. Ono, MercuryII-mediated formation of thymine–HgII–thymine base pairs in DNA duplexes, J. Am. Chem. Soc. 128 (2006) 2172–2173.
[48] X.W. He, N. Ma, A general strategy for label-free sensitive DNA detection based on quantum dot doping, Anal. Chem. 86 (2014) 3676–3681.
[49] S. Tyaji, F.R. Kramer, Molecular beacons: probes that fluoresce upon hybridization, Nat. Biotechnol. 14 (1996) 303–308.
[50] S.A.E. Marras, Selection of fluorophore and quencher pairs for fluorescent nucleic acid hybridization probes, Methods Mol. Biol. 335 (2006) 3–16.
[51] C.Y. Yang, C. Medley, W.H. Tan, Monitoring nucleic acids using molecular beacons, Curr. Pharm. Biotechnol. 6 (2005) 445–452.
[52] Y. Wei, C. Cao, R. Jin, C.A. Mirkin, Nanoparticles with raman spectroscopic fingerprints for DNA and RNA detection, Science 297 (2002) 1536–1540.

Please cite this article in press as: G.-L. Wang, et al., Label-free colorimetric sensor for mercury(II) and DNA on the basis of mercury(II) switched-on the oxidase-mimicking activity of silver nanoclusters, Anal. Chim. Acta (2015), http://dx.doi.org/10.1016/j.aca.2015.02.027